RESEARCH PAPER

OncoImmunology 2:9, e26137; September 2013; © 2013 Landes Bioscience

Early onset and enhanced growth of autochthonous mammary carcinomas in C3-deficient Her2/neu transgenic mice

Silvio Bandini[1,†], Claudia Curcio[2,†], Marco Macagno[1], Elena Quaglino[1], Maddalena Arigoni[1], Stefania Lanzardo[1], Albana Hysi[2], Giuseppina Barutello[1], Lorena Consolino[1], Dario Livio Longo[1], Piero Musiani[2], Guido Forni[1], Manuela Iezzi[2], and Federica Cavallo[1,*]

[1]Department of Molecular Biotechnology and Health Sciences; Molecular Biotechnology Center; University of Torino; Torino, Italy; [2]Aging Research Center; G. D'Annunzio University Foundation; Chieti, Italy

[†]These authors equally contributed to this work

Keywords: complement; genetically engineered mice; Her2/neu; immunosurveillance; mammary cancer

Abbreviations: ADC, apparent diffusion coefficient; αSMA, α-smooth muscle actin; C3, complement component 3; CR3, complement receptor 3; DCE-MRI, dynamic contrast enhanced magnetic resonance imaging; FoxP3, forkhead box P3; IL-1β, interleukin 1β; IFNγ, interferon γ; KO, knockout; Ktrans, volume transfer constant; MCP-1/CCL2, monocyte chemoattractant protein 1; MDSC, myeloid-derived suppressor cell; NK, natural killer; TNFα, tumor-necrosis factor α; Treg, regulatory T cell; VEGF, vascular endothelial growth factor; Vp, plasmatic volume

Aside from its classical role in fighting infections, complement is an important, although poorly understood, component of the tumor microenvironment. In particular, the tumor growth-regulatory activities of complement remain under debate. To assess the role of the complement system in the progression of autochthonous mammary carcinomas, we have crossed complement component 3 (C3)-deficient (*C3*$^{-/-}$) BALB/c male mice with BALB/c females expressing the activated rat *Her2/neu* oncogene (neuT). Although neuT transgenic mice develop spontaneous mammary cancers with 100% penetrance, a significantly shorter tumor latency (i.e., earlier onset of the first palpable tumor), a higher frequency of multiple tumors (multiplicity), and a dramatic increase in the tumor growth rate were found in neuT-*C3*$^{-/-}$ animals. The accelerated tumor onset observed in neuT-*C3*$^{-/-}$ mice was paralleled by an earlier onset of spontaneous lung metastases and by an increase in Her2 expression levels, primarily on the surface of tumor cells. The percentage of immune cells infiltrating neuT carcinomas was similar in C3-deficient and C3-proficient mice, with the exception of a significant increase in the frequency of regulatory T cells in neuT-*C3*$^{-/-}$ tumors. Of particular interest, the enhanced immunosuppression imparted by C3 deficiency clearly influenced the immunogenic phenotype of autochthonous mammary tumors as neuT-*C3*$^{-/-}$ malignant cells transplanted into syngeneic immunocompetent hosts gave rise to lesions with a significantly delayed kinetics and reduced incidence as compared with cells obtained from neuT C3-proficient tumors. Finally, increased blood vessel permeability was evident in neuT-*C3*$^{-/-}$ tumors, although a similar number of tumor vessels was found in neuT and neuT-*C3*$^{-/-}$ lesions. Altogether, these data suggest that complement plays a crucial role in the immunosurveillance and, possibly, the immunoediting of Her2-driven autochthonous mammary tumors.

Introduction

There is a growing body of evidence that suggests that the host immune system plays an important role in modulating the development and spread of cancer, particularly in its early stages. Many of the cellular and molecular mechanisms by which immunological processes exhibit enhancing[1,2] and hampering[3–5] effects on the preliminary stages of neoplastic growth have been worked out in detail.

Complement is a critical participant of innate immune defense systems. Moreover, complement activation products and membrane-bound regulators interact with cells of the adaptive immune response. Such immunological effector functions in eliciting host defense and inflammation can also foster a role for complement in tumorigenesis. Complement activation and signaling mechanisms can be triggered at the site of tumor development by damage-associated molecular pattern (DAMPs) or upon the infiltration of inflammatory cells expressing complement

*Correspondence to: Federica Cavallo; Email: federica.cavallo@unito.it
Submitted: 07/21/2013; Revised: 08/12/2013; Accepted: 08/12/2013
Citation: Bandini S, Curcio C, Macagno M, Quaglino E, Arigoni M, Lanzardo S, Hysi A, Barutello G, Consolino L, Longo D, et al. Early onset and enhanced growth of autochthonous mammary carcinomas in C3-deficient Her2/neu transgenic mice. OncoImmunology 2013; 2:e26137; http://dx.doi.org/10.4161/onci.26137

components.[6–8] Spontaneous antitumor antibodies also play an important role in mediating complement activation at the tumor site.[9–11] Nevertheless, the role of the complement in tumor growth and metastatic spread has not yet been sufficiently explored, and contradictory findings have been reported so far.[12,13] Previous research has primarily evaluated the growth of transplantable tumors in complement-deficient mice, while very few data[14] exist about the influence of complement on the development of autochthonous tumors.

Genetically engineered mice that spontaneously develop tumors as a consequence of defined genetic alterations, typically upon the artificial insertion of exogenous DNA sequences into their genome, allow scientists to study the progressive stages of carcinogenesis and the natural occurrence of cancer.[15,16] These mice are of special interest when they develop tumors that recapitulate both the molecular and genetic changes found in human cancers. The slow tumor progression, the natural occurrence of invasion and metastasis, and the presence of a long-lasting interaction between the tumor, its environment and the host immune system, allow indeed for a direct assessment of the relative contribution of immune mechanisms to both the pace of oncogenesis and the intensity of the forthcoming metastatic spread.[17] One such model permitting analysis of the progressive stages of mammary neoplasia is provided by female transgenic mice expressing the activated rat Her2/neu oncogene under the transcriptional control of the mouse mammary tumor virus promoter (neuT mice).[18] This transgenic mammary adenocarcinoma mouse model is particularly pertinent to human diseases in that it mimics several features of the devastating progression and metastatic capabilities of HER2$^+$ breast cancer in women.[17] From the 4th week of life, cells in the rudimentary mammary ducts of neuT juvenile females start to express Her2/neu, proliferate and form side buds. These initial lesions appear as foci of atypical hyperplasia that gradually coalesce to give rise to large carcinomas in situ, followed by the development of invasive (and ultimately metastatic) carcinomas. The shift from pre-neoplastic to invasive lesions is associated with a vigorous proliferation of microvessels that express $\alpha_v\beta_3$ integrin.[19] These microscopic lesions become palpable through the skin, and gradually occupy the bulk of the subcutaneous fibroadipose tissue of the mammary pad. Moreover, waves of malignant cells disseminate from the primary lesion to the bone marrow during the 4th to 9th weeks of age. Neoplastic cells also settle in lung capillaries and vessels to form roundish intravascular nodules that eventually invade the parenchyma.[20]

Although the overexpression of activated Her2/neu is sufficient to drive mammary lesions in neuT mice, the pace of tumor progression is significantly influenced by the nature of extracellular matrix,[21,22] by perforin-dependent immunosurveillance,[23] and by the tumor-elicited mechanisms of immunosuppression.[24,25] Disease progression is also modulated by the cytokines in the tumor microenviroment.[26,27] In particular, 4 transcriptional networks centered around interleukin-1 β (IL-1β), tumor necrosis factor α (TNFα), interferon γ (IFNγ), and chemokine (C-C motif) ligand 2 (CCL2, best known as MCP-1) are directly linked to inflammation and become increasingly expressed along with the development and progression of neuT carcinomas.[27] The presence of MCP-1 in the stroma of neuT neoplasms enhances the rate of cancer progression, whereas the process is markedly reduced when neuT mice are crossed with *Ccl2*$^{-/-}$ animals. On the other hand, the tumor-elicited expression of IFNγ plays a inhibitory effect on tumor growth. In line with this notion, neuT lesions developing in *Ifng*$^{-/-}$ mice display intense angiogenesis along with an accelerated disease progression.[26,27]

In the current study, we evaluated the biological consequences of defects in the complement system on mammary oncogenesis by analyzing novel neuT transgenic mice lacking the complement component 3 (neuT-*C3*$^{-/-}$ mice). The early onset and accelerated progression of mammary cancer observed in these mice demonstrated that the complement naturally functions to attenuate the growth of Her2/neu$^+$ autochthonous mammary lesions. This protective effect of the complement system appears to rest on multiple factors, including the inhibition of Her2/neu expression by tumor cells as well as of their proliferative potential, a reduction in local immunosuppressive mechanism and alterations in tumor vascularization. In addition, neuT tumors arising in *C3*$^{-/-}$ mice are more immunogenic than those developing in C3-proficient animals. Taken together, our findings indicate that the complement system is involved in the immunosurveillance of Her2$^+$ tumors.

Results

Spontaneous antitumor antibodies increase during cancer progression in neuT mice

As cancer progresses, tumor epitope-reactive antibodies able to specifically bind neoplastic cells are frequently found in cancer patients.[9–11] These anticancer antibodies are among the main mechanisms by which the complement system is activated at the tumor site.[9] We thus evaluated whether antibodies capable of binding cultured neuT-expressing TUBO cancer cells are present in the sera of neuT mice (**Fig. 1A**). Thus, sera were collected from neuT mice at various time points post-birth to evaluate antibody reactivity at distinct tumor developmental stages, including mammary gland diffuse atypical hyperplasia lesions (weeks 8–10), small multifocal carcinomas (weeks 13–15) and large coalescing invasive carcinomas (weeks 19–21 and 34). Cytofluorometric studies upon staining with anti-IgM antibodies showed that early in tumor development the relative amount of TUBO-reactive circulating antibodies in neuT and wild type BALB/c mice is comparable, with both groups exhibiting low levels at 8–10 and 13–15 weeks of age. However, TUBO-reactive antibodies significantly increased ($P < 0.03$) in the sera of neuT (but not of wild-type BALB/c) mice in the course of disease progression, starting as early as 19–21 weeks post-birth and increasing further at 34 weeks. A similar pattern was found in neuT-*C3*$^{-/-}$ mice, with sera from 19–21 week-old females displaying approximately double the amount of TUBO-binding antibodies than sera from 13–15 week-old animals. Moreover, a significant increase of spontaneous antitumor antibodies was observed in sera from 19–21 week-old neuT-*C3*$^{-/-}$ mice as compared with those of age-matched neuT animals (**Fig. 1A**).

Deposition of C3 fragments occurs in neuT carcinomas

Spontaneous antibodies directed against tumor-associated antigens can trigger complement activation at the tumor site. To

evaluate whether complement activation occurs in the mammary glands of neuT mice in the course of tumor progression, we monitored the presence of C3 fragments in the mammary neoplasms by confocal immunofluorescence microscopy (**Figure 1B**). Upon staining with an anti-C3b/iC3b/C3c antibody, C3 cleavage products were clearly evident in the tumor vasculature and stroma of mammary neoplasms developing in neuT mice (**Fig. 1B**, left panel), whereas they were absent, as expected, from neuT tumors arising in *C3*$^{-/-}$ animals (**Fig. 1B**, right panel). While C3 cleavage provides evidence that the initial steps of complement activation occur at the tumor site, potentially leading to the generation of complement effectors, it remains uncertain whether this actually results in the assembly of the membrane attack complex on neuT tumor cells. In this regard, we have observed that neuT cancer cells that harbor high levels of Her2/neu on their surface also express elevated levels of the decay-accelerating factor (CD55; **Fig. S1**).

The onset of autochthonous Her2/neu-driven carcinomas is accelerated in neuT-C3$^{-/-}$ mice

To assess whether the marked complement activation occurring at the tumor site affects the development of mammary lesions, we compared mammary tumor onset and growth in neuT and neuT-*C3*$^{-/-}$ mice (**Fig. 2A–C**). In neuT-*C3*$^{-/-}$ mice, an early onset of the first palpable lesions ($P = 0.0001$; **Figure 2A**) and higher mean tumor multiplicity (P ranging from 0.02 to < 0.0001; **Figure 2B**) were found as compared with neuT mice. An earlier incidence and an elevated tumor multiplicity were also evident in C3 heterozygous neuT-*C3*$^{+/-}$ mice, relative to neuT controls (**Fig. S2**). Moreover, tumors arising in neuT-*C3*$^{-/-}$ mice grew faster than those arising in neuT mice, achieving a predetermined tumor volume in a significantly shorter period of time ($P < 0.0001$; **Figure 2C**). A comparative whole mount microscopic analysis of the mammary glands showed that the progression from hyperplastic lesions to in situ carcinoma and invasive solid carcinomas is accelerated in neuT-*C3*$^{-/-}$ mice (**Fig. 2D–I**). While large microscopic lesions (equivalent to in situ carcinomas) become evident only from the 15th and 17th week of age in neuT mice (**Fig. 2D–F**), they are already evident as early as 11 weeks of age in neuT-*C3*$^{-/-}$ mice (**Fig. 2G**). By week 15, neuT-*C3*$^{-/-}$ lesions are notably enlarged (**Fig. 2H**) and at week 17 their further expansion and clumping occupy the whole mammary gland (**Fig. 2I**). Despite their different growth kinetics, carcinomas developing in neuT and neuT-*C3*$^{-/-}$ displayed a similar grade of differentiation (**Fig. 2J and L**).

The accelerated tumor onset observed in neuT-*C3*$^{-/-}$ mice was paralleled by the earlier onset of spontaneous lung metastases (**Table 1**; **Figure 2K and M**), which were evident at week 15 (when the lungs of all neuT mice were still free of metastases). Altogether, these data point to the crucial role of C3 in hampering Her2/neu-driven autochthonous mammary carcinomas.

Accelerated carcinoma progression in neuT-*C3*$^{-/-}$ mice is associated with increased Her2/neu expression

As compared with mammary lesions arising in neuT mice, tumors evolving in neuT-*C3*$^{-/-}$ mice displayed an abundant expression of the proliferation marker proliferating cell nuclear antigen (PCNA; **Figure 3A–C**). This is in line with the accelerated growth rate of clinically evident carcinomas (**Fig. 2C**). Since Her2/neu is the driving force behind neuT tumors, we compared Her2/neu expression levels in tumors developing in neuT and neuT-*C3*$^{-/-}$ mice. Immunoblotting

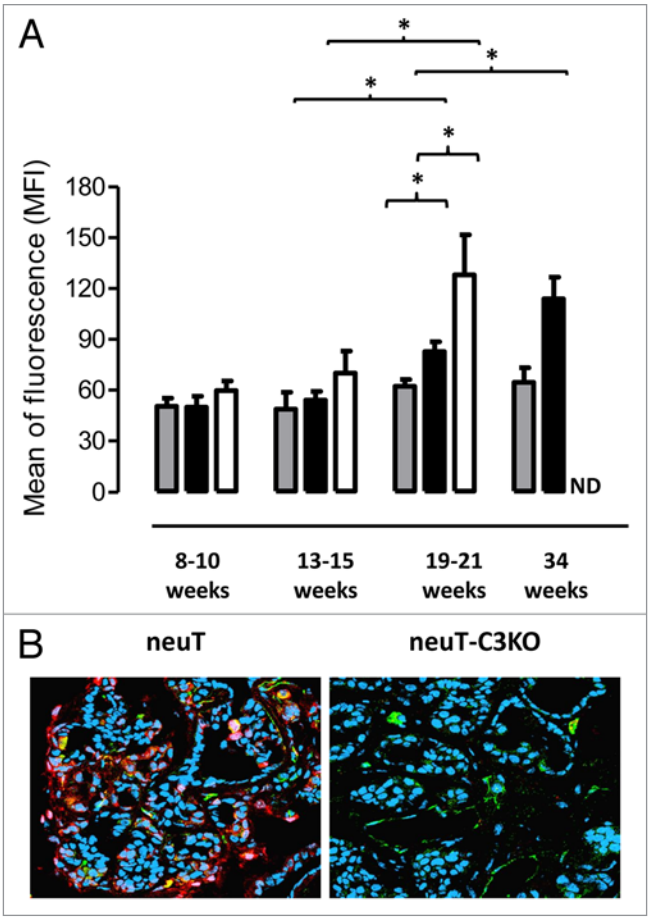

Figure 1. Increase in circulating spontaneous antitumor antibodies and C3 fragment deposition in mammary tumor lesions in neuT mice. (**A**) Titers of antibody recognizing TUBO cells in the sera of 8–10, 13–15, 19–21, and 34 week-old BALB/c (n = 6–10; gray bars), neuT (n = 6–11; black bars) and neuT-*C3*$^{-/-}$ (n = 6–12; white bars) mice. TUBO cells were incubated in the presence of diluted sera and antibodies binding to the TUBO cells were detected upon staining with fluorescent anti-IgM antibodies and flow cytometry. Results are expressed as MFI (mean ± SEM n = 4 independent experiments). *$P = 0.03$, 2-tailed Student t-test. (**B**) Confocal microscopy of frozen tumor sections labeled with anti-C3b/iC3b/C3c antibodies (red), anti-CD31 antibodies (green) and TO-PRO$^{®}$-3 iodide (blue, recognizing nuclei). Original magnification, × 400. Images are representative of 10 neuT and neuT-*C3*$^{-/-}$ tumors analyzed.

Table 1. Spontaneous metastatic spread to the lungs of neuT and neuT-*C3*$^{-/-}$ mice

Mice	Week 15	Week 17	Week 20	Week 25
neuT	0%[a] (0/15)[b]	0% (0/14)	0% (0/6)	100% (5/5)
neuT-*C3*$^{-/-}$	11% (1/9)	25% (2/8)	40% (3/9)	100% (5/5)

[a]percentage of mice with lung metastases. [b]number of mice with lung metastases/total mice.

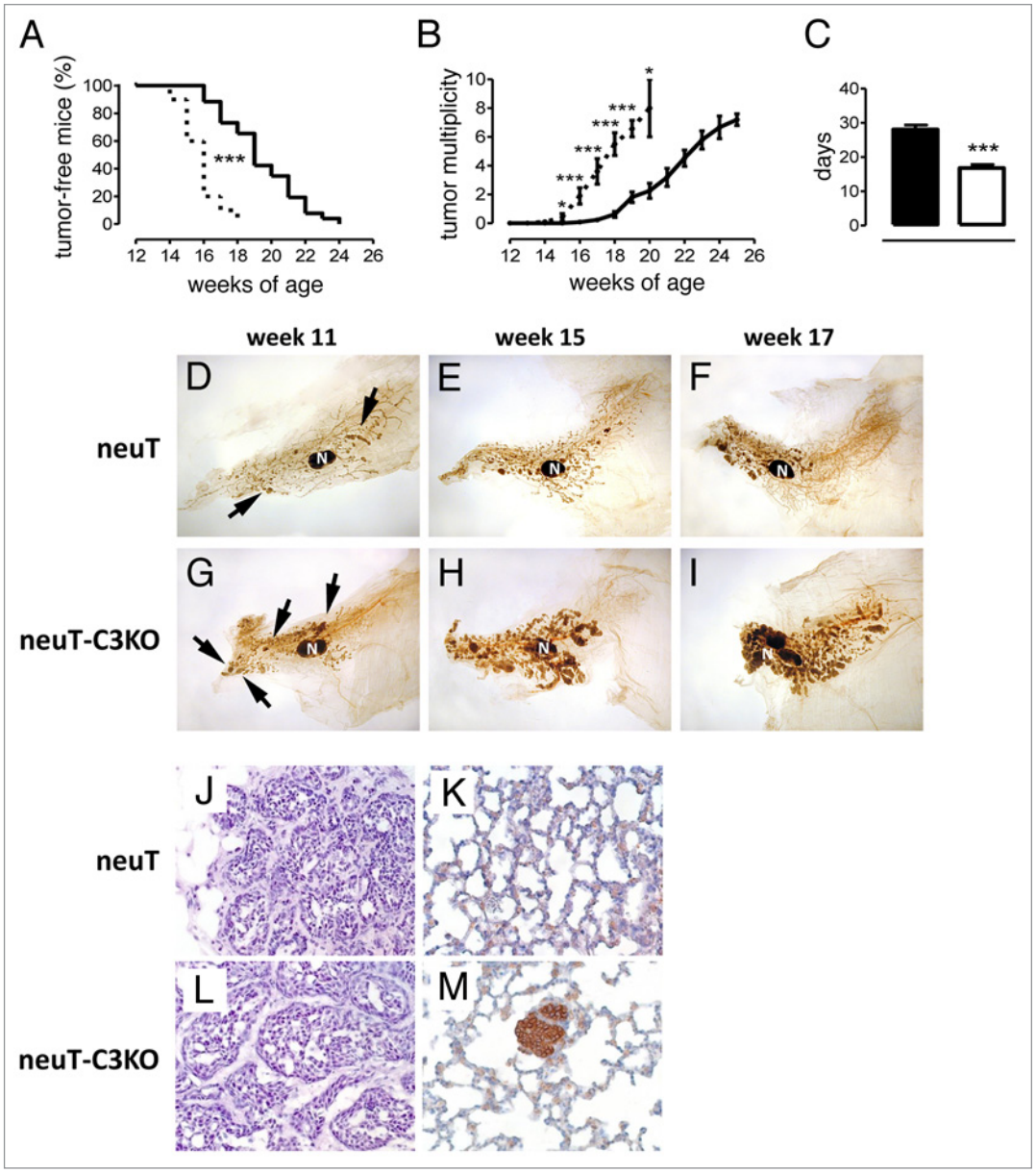

Figure 2. Accelerated pace of autochthonous Her2/neu-driven mammary carcinogenesis and metastatic spread in neuT-*C3*$^{-/-}$ mice. Incidence (**A**), and multiplicity (**B**) of mammary carcinomas in female neuT (n = 26, continuous line) or neuT-*C3*$^{-/-}$ mice (n = 10, dashed line). Earlier incidence (***P = 0.0001, Log-rank Mantel-Cox Test) and higher tumor multiplicity (*P = 0.02; **P = 0.004; ***P < 0.0001, 2-tailed Student t-test) were found in neuT-*C3*$^{-/-}$ mice. (**C**) Time (days) required for a 2-mm (mean diameter) tumor to reach an 8-mm threshold in neuT-*C3*$^{-/-}$ (white bar) vs. neuT (black bar) mice. ***P < 0.0001, 2-tailed Student's t-test. (**D–I**) Whole mount microscopic analysis of the fourth (inguinal) mammary gland. The large central oval black spot in each image is the intra-mammary lymph node (N). Arrows indicate multifocal hyperplastic lesions appearing as black spots with a relatively round shape along the path and within the mammary ducts. Tumor progression in neuT mice (**D–F**) is accelerated in neuT-C3KO mice with extended hyperplastic foci and small in situ tumors evident at 11 weeks of age (**G**), small palpable tumors at 15 weeks (**H**) and large lesions and tumor masses filling most of the mammary fat pad at week 17th (**I**). Magnification 6.3×. (**J–M)** Histological (H&E, left panels) and immunohistochemical (Her2, right panels) staining of mammary tumor lesions (**J and L**) and lungs (**K and M**) from 17 week-old neuT and neuT-C3KO mice. Magnification 400X.

studies revealed a more prominent Her2/neu band in tumor cell lysates from neuT-*C3*$^{-/-}$ mice, and quantification showed that Her2/neu protein levels were 6–8-fold higher in neuT-*C3*$^{-/-}$ than in neuT tumors (**Fig. 3D**). On confocal microscopy, Her2/neu appeared to be focally expressed mainly at the cell membrane of tumor cells, with individual cells staining with varying intensities (**Fig. 3E–G**; **Fig. S1**). Her2/neu was even more readily detectable in neuT-*C3*$^{-/-}$ cancer cells, exhibiting both higher Her2/neu levels and a more homogeneous expression than neuT cells (**Fig. 3H–J**; **Fig. S1**). These data suggest that C3 cleavage at the tumor site triggered by spontaneous antibodies directed against Her2/neu and/or other tumor-associated antigens may limit Her2/neu expression with a corresponding reduction in the proliferative ability of neuT tumor cells.

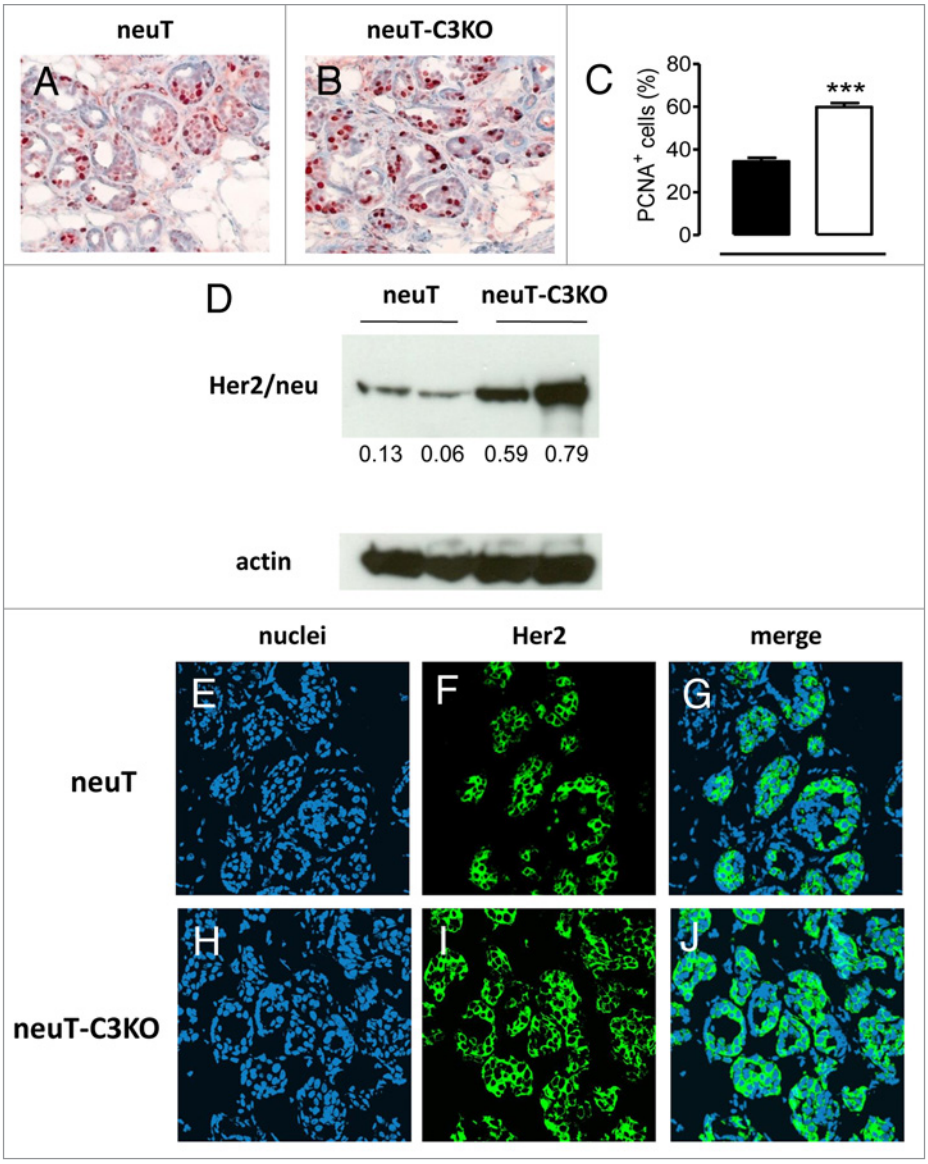

Figure 3. Increased expression of proliferation markers and Her2/neu in neuT-*C3*$^{-/-}$ mammary cancer cells. (**A-B**) Immunohistochemical staining of tumor cryosections from neuT (A) or neuT-*C3*$^{-/-}$ mice (B) with anti-PCNA antibody. Magnification 400X. Results are representative of 10 neuT and 10 neuT-*C3*$^{-/-}$ tumors. (**C**) Percentage of PCNA^{+} cells from neuT (black bar) and neuT-*C3*$^{-/-}$ mice (white bar) tumors (quantification of staining in **A and B**, n = 10 per group and 5 fields per tumor). *** $P < 0.0001$, 2-tailed Student t-test. (**D**) Her2/neu (upper panel) and actin (lower panel) protein levels as measured by immunoblotting in mammary glands from neuT (lane 1 and 2) and neuT-*C3*$^{-/-}$ (lane 3 and 4) carcinoma. The numbers under each lane indicate the ratios between Her2/neu and actin levels as measured by densitometry using the Quantity One software. 3 independent experiments were performed and a single representative image is shown. (**E-J**) Confocal microscopy of frozen tumor sections from neuT and neuT-*C3*$^{-/-}$ mice (n = 8 per group) labeled with anti-Her2 antibodies (green) and TO-PRO®-3 iodide (blue, labeling nuclei). Original magnification, 400X.

The tumor microenvironment in neuT-*C3*$^{-/-}$ mice is more immunosuppressive than that of neuT mice

We next sought to evaluate whether C3 defects also have an impact on the composition of tumor-infiltrating leukocytes. C3 deficiency did not alter the percentages of either circulating or tumor-infiltrating leukocytes, as shown by white blood cell counts (**Fig. S3**) and immunohistochemistry (**Fig. S4**), respectively. No significant differences in the frequency of tumor-infiltrating macrophage, CD4^{+} and CD8^{+} T lymphocytes, B cells and myeloid-derived suppressor cells (MDSCs) were found in tumors arising in neuT and neuT-*C3*$^{-/-}$ mice by cytofluorometric analysis (**Fig. 4A**). The amount of splenic MDSCs was also similar irrespective of C3 status (**Fig. S5A**). In contrast, the frequency of regulatory T cells (Tregs) was significantly increased ($P = 0.02$) in neuT-*C3*$^{-/-}$ mice tumors relative to neuT neoplasms (**Fig. 4B**), with a similar trend evident in splenocyte preparations (**Fig. S5B**). The increase in Tregs was confirmed by immunohistochemistry, showing that forkhead box P3 (FoxP3)$^{+}$ cells are comparatively more abundant in neuT-*C3*$^{-/-}$ tumors (**Fig. 4C**). This finding is in line with the notion that a reduced signaling through the receptors for the complement fragments C3a and C5a supports the development of

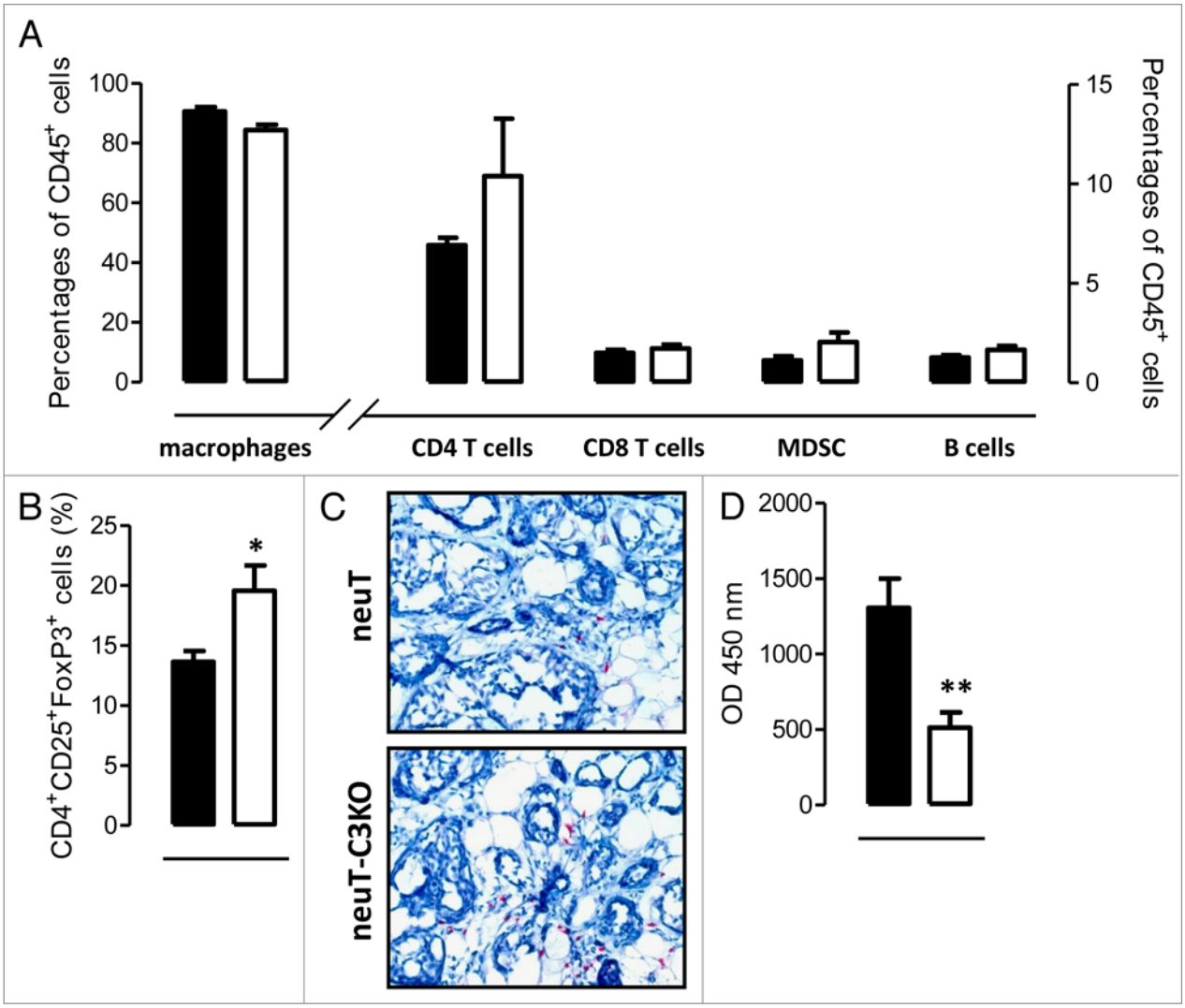

Figure 4. Autochthonous mammary tumors from neuT-*C3*$^{-/-}$ mice have a more immunosuppressive microenvironment as compared to that of neuT mice. (**A and B**) Lymphocyte infiltrates in neuT and neuT-*C3*$^{-/-}$ tumors were analyzed by flow cytometry. Mammary tumors from neuT (n = 6; black bars) and neuT-*C3*$^{-/-}$ (n = 7; white bars) mice were dissociated and tumor cells were stained for the assessment of CD45, CD11b, F4/80, CD3, CD4, CD8, Gr-1, and B220 (**A**) or CD3, CD25, CD4, and FoxP3 (**B**) expression. (**A**) CD45$^+$ leukocytes were gated and various immune cell subsets were identified as follows: macrophages: CD11b$^+$F4/80$^+$; CD4$^+$ T cells; CD3$^+$CD4$^+$; CD8$^+$ T cells: CD3$^+$CD8$^+$; B cells: B220$^+$CD11b$^-$. CD45$^+$CD11b$^+$ leukocytes were gated and myeloid-derived suppressor cells (MDSCs) were identified as GR-1$^+$ cells within that subset. (**B**) CD3$^+$ leukocytes were gated and regulatory T cells (Tregs) were identified as CD4$^+$CD25$^+$FoxP3$^+$. Bars represent the percentage of positive cells ± SEM. 4 independent experiments were performed and a single representative image is shown. (**C**) Immunohistochemical staining of neuT and neuT-*C3*$^{-/-}$ mammary tumors for FoxP3 expression, showing a prominent increase in FoxP3$^+$ cells in the tumor stroma. Results are representative of 8 of each neuT and neuT-*C3*$^{-/-}$ tumors analyzed. (**D**) Sera from 15–17 weeks-old neuT (n = 13; black bar) and neuT-*C3*$^{-/-}$ (n = 12; white bar) mice were tested for C5a levels by ELISA. 3 independent experiments were performed and a single representative example is shown. Results are expressed as mean ± SEM of the optical density (OD). *P = 0.02; **P = 0.002, 2-tailed Student t-test.

FoxP3$^+$ Tregs.[28] These same complement receptors have also been shown to limit the functions of naturally occurring Tregs.[29] Of note, C3a cannot be generated in neuT-*C3*$^{-/-}$ mice, while C5a is present, albeit at strongly reduced levels as compared with neuT mice (P = 0.002, **Fig. 4D**).

Carcinomas arising in neuT-*C3*$^{-/-}$ mice are more immunogenic than those growing in neuT mice

To assess whether the increased frequency of tumor-infiltrating Tregs caused by the absence of C3 can influence the immunogenic phenotype of Her2/neu-driven autochthonous tumors, the tumorigenicity of mammary carcinomas from neuT and neuT-*C3*$^{-/-}$ mice was compared by means of transplantation experiment. Upon transplantation into naïve syngeneic immunocompetent hosts, cancer cells isolated from neuT-*C3*$^{-/-}$ mice generated lesions with a reduced efficiency, a long latency (**Fig. 5A**) and a slow kinetic (**Fig. 5B**) as compared with those from neuT mice. Similar results were found when the same tumor cells were injected into *C3*$^{-/-}$ BALB/c mice (**Fig. 5C and D**). Altogether, these data suggest that tumors from *C3*$^{-/-}$ mice undergo limited levels of immunoediting as are therefore relatively more immunogenic. Moreover, since malignant cells obtained from neuT mice generated tumors with significantly shortened delays in

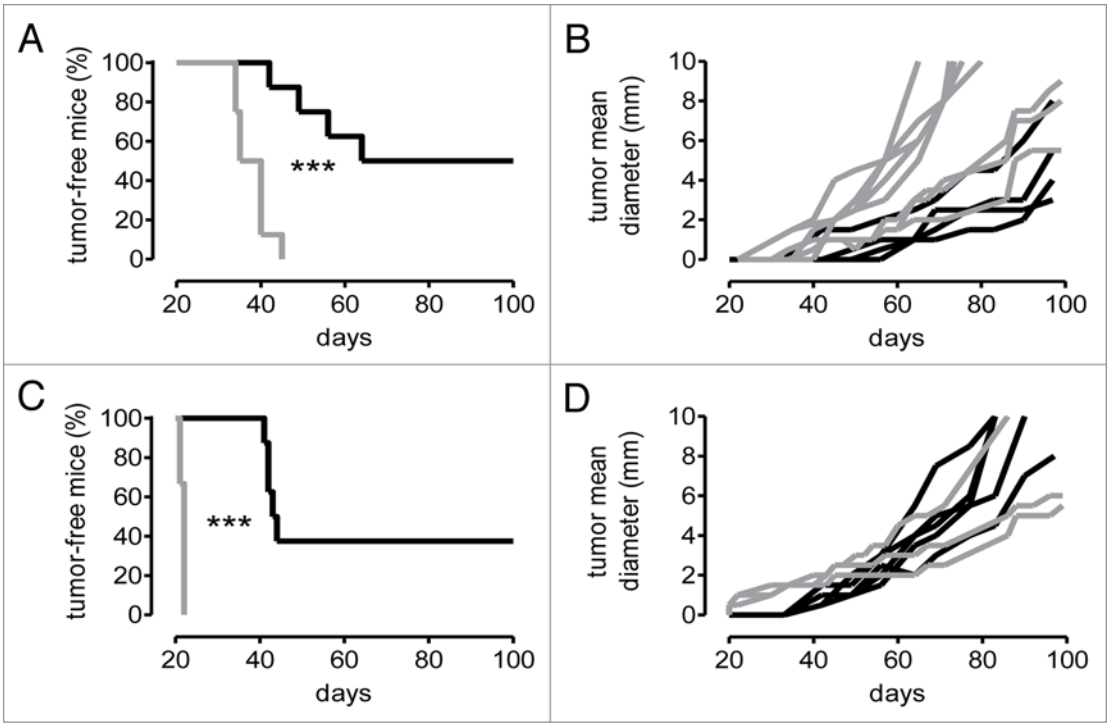

Figure 5. Increased immunogenicity of neuT-*C3*$^{-/-}$ tumors. (**A and B**) Incidence (**A**), and tumor growth (**B**) of 1 × 10^6 mammary carcinoma cells dissociated from neuT (gray lines) and neuT-*C3*$^{-/-}$ (black lines) donor mice and injected subcutaneously into immunocompetent BALB/c females (n = 8 per group). (**A**) Reduced (50%) and delayed incidence (***P < 0.0001, Log-rank Mantel–Cox Test) was found upon transplantation of tumor cells from neuT-*C3*$^{-/-}$ as compared with cells from neuT mice. (**B**) Tumor growth plotted as mean tumor diameter over time. Each line refers to an individual tumor. 5 independent experiments were performed and a single representative example is shown. (**C and D**) Incidence (**C**), and tumor growth (**D**) of mammary carcinomas from neuT (n = 3; gray lines) and neuT-*C3*$^{-/-}$ mice (n = 8; black lines) injected subcutaneously to *C3*$^{-/-}$ females. (**C**) Reduced (62.5%) and delayed incidence (***P = 0.0008, Log-rank Mantel–Cox Test) was observed for neuT-*C3*$^{-/-}$ cells. (**D**) Tumor growth plotted as mean tumor diameter over time. Each line refers to an individual tumor. Three independent experiments were performed and a single representative example is shown.

C3$^{-/-}$ (**Fig. 5C**) as opposed to fully immunocompetent (**Fig. 5A**) mice, C3 also appears to counteract the growth of immunoedited tumors.

Tumor vessels in *C3*$^{-/-}$ mice are enlarged and display increased permeability

The increased proliferative ability of *C3*$^{-/-}$ cancer cells and their capacity to establish an immunosuppressive microenvironment likely accounts for the earlier incidence and accelerated growth of Her2/neu-induced carcinomas in neuT-*C3*$^{-/-}$ mice. However, a rapidly growing cancer needs a correspondingly large blood supply. Because complement is known to play an important role in modulating vascularization and angiogenesis,[14,30] we evaluated tumor microvascular density by endothelial cell staining in neuT (**Fig. 6A**) and neuT-*C3*$^{-/-}$ (**Fig. 6B**) tumors of equivalent size.

Although similar numbers of intratumoral vessels were found in neuT and neuT-*C3*$^{-/-}$ carcinomas (**Fig. 6C**), tumor-associated vessels in neuT neoplasms (**Fig. 6A**) appeared to be thinner than those of neuT-*C3*$^{-/-}$ lesions (**Fig. 6B**). A statistical assessment of vessel diameter confirmed that tumor-associated blood vessels are significantly larger in carcinomas developing in the absence of C3 (**Fig. 6D**). The large diameter of intratumoral vessels observed in neuT-*C3*$^{-/-}$ carcinomas correlated with an increased number of Ng2$^+$ pericytes in association with endothelial cells (**Fig. 6E and F**). The small increase in Ng2$^+$ pericytes in the vasculature of neuT-*C3*$^{-/-}$ tumors became more readily apparent by visualizing only mature pericytes upon staining with an antibody specific for α-smooth muscle actin (αSMA; **Figure 6G and H**). The higher frequency of αSMA$^+$ mature pericytes in neuT-*C3*$^{-/-}$ carcinomas indicates that the lack of C3 promotes the pericyte investment of endothelial cells and, in a more marked way, their maturation.

Since tumor-induced angiogenesis is largely dependent on vascular endothelial growth factor (VEGF), and neuT carcinomas produce VEGF,[26,31] we analyzed serum VEGF levels in neuT and neuT-*C3*$^{-/-}$ mice. A significant increase in VEGF levels coincident with the expansion of mammary lesions was observed in both neuT and neuT-*C3*$^{-/-}$ mice. However, no significant differences were found in the relative amounts of VEGF in neuT and neuT-*C3*$^{-/-}$ mice with the same tumor burden (**Fig. 6I**). This finding is consistent with the observation that neuT and neuT-*C3*$^{-/-}$ mice exhibit equivalent numbers of tumor-associated blood vessels. The low diameter and reduced area of the vessels serving neuT carcinomas can therefore be ascribed to the direct effect of complement deposition on endothelial cells.[32]

Finally, we utilized dynamic contrast enhanced magnetic resonance imaging (DCE-MRI) to assess whether the large diameter of tumor-associated vessels found in neuT-*C3*$^{-/-}$ carcinomas coupled to their mature and stable phenotype result in

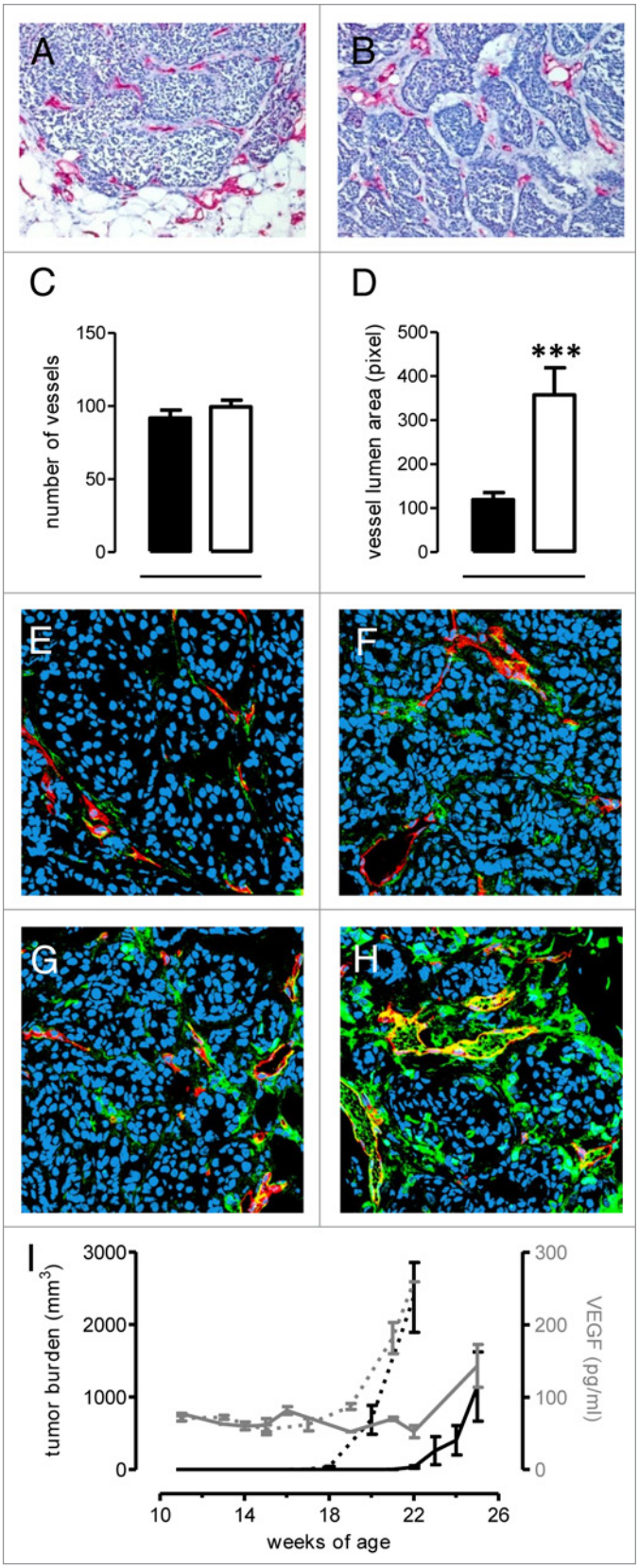

Figure 6. C3 deficiency does not modify absolute blood vessel number but changes vessel architecture. (**A–B**) Immunohistochemical staining of cryosections for endothelial cell markers (CD31 and CD105, red) to visualize blood vessels in mouse tumors of equal volume developed in neuT (**A**) and neuT-*C3*$^{-/-}$ (**B**) mice. (**C–D**) Quantification of the number (**C**) and lumen area (**D**) of vessels in neuT (black bar) and neuT-*C3*$^{-/-}$ (white bar) carcinoma. Results are represented as means ± SEM from 7 ×100 microscopic fields of 10 tumors. (**E–H**) Confocal microscopy analysis of samples stained with anti-CD31 antibodies (red) and anti-Ng2 antibody (**E and G**, green) or anti-SMA antibodies (**F and H**, green) in neuT (**E and F**) or neuT-*C3*$^{-/-}$ (**G and H**) tumors. (**I**) Circulating levels of vascular endothelial growth factor in neuT (n = 5, continuous gray line) and neuT-*C3*$^{-/-}$ (n = 6, dotted gray line) mice were evaluated by ELISA and plotted together with mice tumor burden (continuous black line and dotted black line for neuT and neuT-*C3*$^{-/-}$ mice, respectively). A statistically significant (***P = 0.0002 between week 22 and 25 for neuT mice and ***P = 0.0003 between week 19 and 21 for neuT-*C3*$^{-/-}$ mice) increase in serum VEGF along with tumor progression was observed in both neuT and neuT-*C3*$^{-/-}$ mice.

major functional differences in the vasculature. The quantitative analysis of intratumoral DCE-MRI images showed that the vessel permeability of neuT-*C3*$^{-/-}$ carcinomas is enhanced relative to that of neuT neoplasms (**Fig. 7A**, volume transfer constant Ktrans = 8.2 × 10^{-5} and 1.6 × 10^{-4} for neuT and neuT-*C3*$^{-/-}$ lesions, respectively). Similarly, carcinomas from neuT-*C3*$^{-/-}$ mice displayed a markedly higher plasmatic volume (Vp) reflecting the increased percentage of tumor mass occupied by vessels (**Fig. 7B**, Vp = 0.012 and 0.035 for neuT and neuT-*C3*$^{-/-}$ lesions, respectively, P = 0.05). Considering the amount of extravasation of injected contrast agent, we found broad regions showing low (if any) contrast enhancement in neuT carcinomas, paralleling a relatively high necrotic index (**Fig. 7C**, 53.3% and 30.6% for neuT and neuT-*C3*$^{-/-}$ lesions, respectively). Moreover, the mean apparent diffusion coefficient (ADC) of neuT-*C3*$^{-/-}$ tumors was higher than that of neuT tumors (**Fig. 7D**, 8.6 × 10^{-4} and 1.1 × 10^{-3} mm^2/sec, respectively). This disparity presumably originates from differences in the composition of the stromal space surrounding the blood vessels in the presence and absence of C3. Alternatively, this discrepancy may be related to the unique cellularity in the tumor microenvironment resulting from the unequal kinetics of disease progression in neuT and neuT-*C3*$^{-/-}$ mice.

Discussion

Although multiple mechanisms by which various aspects of the immune system may either enhance or impair tumor development have been precisely delineated, the role of complement in this respect has been relatively under-explored. Currently available data are contradictory, with a few studies pointing to a protective function for the complement in the host response against malignant cells,[6,28,33] and others highlighting potential tumor-promoting activities of the complement system.[14,34–37] This discordance is not surprising in view of the fact that the complement functionally contributes to a plethora of distinct immunological and inflammatory processes,[13] each of them having unique context-dependent outcomes in different tumor models. In the present study, we have gathered new information to elucidate the role of C3, the central component of the complement cascade, in modulating the development of Her2/neu-driven autochthonous mammary adenocarcinomas in neuT mice. These mice provide a well-defined and progressive model of Her2/neu driven breast cancer.[18]

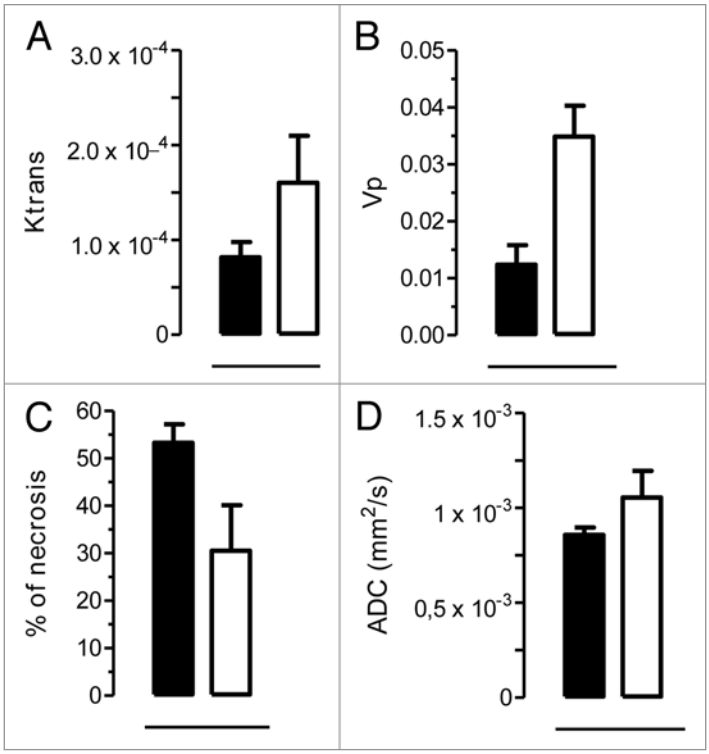

Figure 7. C3 deficiency increases permeability/perfusion and water diffusion in neuT tumors. (**A–C**) MRI evaluation of tumor permeability/perfusion, % of necrosis and water diffusion in mammary tumors from neuT (n = 2; black bars) and neuT-*C3*$^{-/-}$ (n = 2; white bars) mice. Tumor permeability (Ktrans) (**A**) and plasmatic volume (Vp) (**B**) were estimated from DCE-MRI data. The percentage of necrotic tissue was calculated as tumor regions showing contrast enhancement lower than 1.5-fold increase in comparison to pre-injection images (**C**). Molecular water diffusion (ADC) values were calculated from DWI images in tumor regions (**D**). Data are expressed as means ± SD.

Here, we show that activated C3 fragments accumulate in the vessels and stroma of the areas of the mammary gland undergoing Her2/neu-driven neoplastic transformation but not in the surrounding tissue. These findings suggest that complement activation occurs in a tumor-specific rather systemic manner. One of the possible mechanisms underlying such a local activation pattern may rely on spontaneous antibodies present in the tumor microenvironment that specifically react with antigens expressed on the surface of cancer cells.[38] In support of this notion, we observed that spontaneous antitumor antibodies increase in neuT mice in the course of tumor progression. Similar observations have been made in cancer patients.[9–11]

To investigate the biological consequences of complement activation in the tumor microenvironment, we crossed neuT mice with *C3*$^{-/-}$ animals. Thus, neuT and neuT-*C3*$^{-/-}$ mice allowed us to comparatively evaluate mammary oncogenesis and tumor progression in the presence and absence of C3. We found that defects in the complement system accelerate Her2/neu-driven tumorigenesis, increase tumor multiplicity, boost tumor growth and promote the metastatic spread of cancer cells to the lungs. Such an aggressive behavior discloses a protective role for complement-dependent mechanisms in the inhibition of Her2/neu-driven carcinogenesis, at least in neuT mice and possibly in human patients.

The aggressive disease progression observed in neuT-*C3*$^{-/-}$ mice does not appear to reflect the lack of a single activity of complement, but rather seems to result from multiple distinct biochemical changes and cellular processes dependent upon C3 activation. First, the dramatic increase in the growth rate of neuT-*C3*$^{-/-}$ carcinomas was paralleled by an increase in Her2/neu expression. This suggests that one of the consequences of C3 activation at the tumor site is the downregulation of Her2/neu. This is actually one of the direct mechanisms by which anti-Her2/neu antibodies inhibit disease progression in neuT mice.[39,40] Spontaneous antitumor antibodies, some of which are probably directed against Her2/neu epitopes, were found here to accumulate in the course of tumor progression, in both neuT and neuT-*C3*$^{-/-}$ mice. Complement activation may inhibit Her2/neu expression in viable cancer cells, or, alternatively, tumor cells expressing higher levels of Her2/neu could be eliminated following the deposition of C3 as activated by Her2/neu-targeting antitumor antibodies. In this context, the killing of tumor cells probably is not due to the formation of the membrane attack complex, as neuT cancer cells were found to express high levels of CD55, the molecule that is responsible for the accelerated dissolution of C3 and C5 convertases and abrogates the release of anaphylotoxins.[41] An alternative scenario is that C3-coated Her2/neu-overexpressing tumor cells may be killed by natural killer (NK) cells that express integrin α M (Itgam), better known as complement receptor 3 (CR3). CR3, upon stimulation by iC3b, can induce cytotoxic responses in NK cells, especially when MHC class I molecules are poorly expressed by target cells.[42]

Indeed, an inverse correlation exists between the expression levels of Her2/neu and those of MHC class I molecules as well as other components of the antigen-processing machinery.[43] Thus, Her2/neu-overexpressing tumor cells may escape lysis by cytotoxic T lymphocytes, while remaining susceptible to the activity of NK cells. Moreover, signaling via the Her2/Her3 pathway in breast carcinoma cell lines has been shown to improve their recognition by NK and T cells via the killer cell lectin-like receptor subfamily K, member 1 (KLRK1, best known as NKG2D).[44]

Carcinomas developing in neuT-*C3*$^{-/-}$ mice display a marked increase in the frequency of tumor-infiltrating Tregs, possibly contributing to their unhindered expansion. Complement is known to have an integral role in modulating the induction and function of Tregs, thus operating as an important mediator of immunological tolerance.[28,29] During the early steps of T-cell activation, signaling through the C3a and C5a receptors on the surface of CD4$^+$ T cells and dendritic cells (DCs) upregulates the expression of co-stimulatory molecules and increases T-cell survival.[45] Moreover, C3a and C5a receptor signaling modulates the function of circulating Tregs by repressing FoxP3.[29] On the other hand, the absence of such a signal transduction cascade not only deflects naïve T cells into induced Tregs,[28] but also improves the function of naturally occurring Tregs.[29] In neuT-*C3*$^{-/-}$ mice, C3a is not generated but the C5 convertase-like activity of thrombin[46,47] allows for the production of C5a, though in lower amounts than in neuT mice. Consequently, the complete lack of C3a signaling and reduced signaling through the C5a receptor may contribute to the observed increase in Tregs in neuT-*C3*$^{-/-}$ mice.

The highly immunosuppressive tumor microenvironment of neuT-*C3*$^{-/-}$ carcinomas may be instrumental for their escape from the immune system and immunoediting.[48] Accordingly, we observed that neuT-*C3*$^{-/-}$ carcinoma cells display impaired growth upon transplantation into syngeneic immunocompetent BALB/c mice.

Altogether, these data suggest that the complement system is a key factor in the interrelationship between tumor cells and the host immune system, participating in the immunosurveillance and editing of neoplastic lesions, 2 immunological activities that may be sufficient to explain the increased malignancy of cancers developing in neuT-*C3*$^{-/-}$ mice. Nevertheless, beyond its role in immunity, the complement system is also involved in tissue remodeling processes, including neo-angiogenesis.[30] Whether the complement exerts pro- or anti-angiogenic functions is still controversial. Few studies - none of which on breast cancer - have evaluated the role of the complement system in regulating tumor angiogenesis in vivo, yielding contradictory results.[14,36,49] The only study that has evaluated the consequences of the genetic blockade of C3 performed to date[14] reported a reduced microvascular density in tumors developing in *C3*$^{+/-}$ mice, suggesting the existence of a pro-angiogenic function for C3. In the present study, we show that C3 activation on the tumor vasculature impairs angiogenesis. Specifically, we observed no major differences in vascular density between neuT-*C3*$^{-/-}$ and neuT carcinomas. However, the vessels of neuT-*C3*$^{-/-}$ lesions were enlarged and exhibited a mature and functional phenotype, as indicated by the increased number of both young and mature pericytes as well as by increased Vp, as measured by DCE-MRI. Due to their improved structural maturity, ameliorated permeability and diffusion rates, the vessels of *C3*$^{-/-}$ neoplastic lesions provide improved oxygen and nutrient supply, thus fostering rapid tumor growth. In line with this notion, we observed a decrease in necrotic areas within neuT-*C3*$^{-/-}$ neoplasms as compared with neuT lesions.

In conclusion, our data support the notion that the complement system plays a protective role against the development of autochthonous Her2/neu-driven mammary carcinomas in neuT mice. However, as expected for a system with innumerous distinct activities, this protective role does not appear to rest on a single function of crucial importance, but rather on the confluence of multiple distinct activities that together affect the onset and expansion of mammary carcinomas in neuT mice. While our findings should be taken into account from a clinical perspective, such mechanistic complexities may explain why in genetically-engineered mouse model prone to develop ovarian carcinomas, the lack of C3 resulted in an attenuated tumor phenotype and even abrogated oncogenesis and disease progression.[14] It is conceivable that a number of variables, including the genetic background, the nature of the oncogene and its associated promoter, the relative immunological tolerance of the transgene protein product, the resultant tumor type, and the degree of tumor penetrance may all influence how the complement system affects tumor progression, culminating in very different biological outcomes. Nevertheless, defining the molecular peculiarities of this important immunoregulatory factor of the tumor microenvironment may allow the exploitation of complement as a major contributor to immunosurveillance and control of cancer progression in the clinic.

Materials and Methods

Mice

C3$^{-/-}$ BALB/c mice,[50] kindly provided by Prof. Marina Botto (Imperial College, UK), were crossed with Her2/neu transgenic BALB/c (neuT) male mice.[18] Heterozygous C3 and Her2/neu$^+$ (neuT-*C3*$^{+/-}$) male mice were then crossed with *C3*$^{-/-}$ females and the progeny was genotyped in order to identify the *C3*$^{-/-}$ Her2/neu$^+$ males (neuT-*C3*$^{-/-}$) that were subsequently crossed with *C3*$^{-/-}$ females. The neuT-*C3*$^{-/-}$ progeny were used for the experiments as indicated. The mammary glands of all neuT mice were inspected and palpated twice a week for tumor appearance. Individual neoplastic masses were measured with calipers in 2 perpendicular diameters and the average value was recorded. Progressively growing masses > 1 mm in mean diameter were regarded as tumors. Neoplastic growth was monitored until the first tumor that exceeded a mean diameter of 10 mm was found, at which point mice were euthanized for ethical reasons. Tumor multiplicity was calculated as the cumulative number of incident individual tumors/total number of mice and is reported as mean ± SEM. Tumor volume was calculated as $(X^2\ Y) / 2$, where X and Y represent the shortest and longest tumor sizes, respectively. Tumor burden was calculated as the sum of individual tumor

volumes of each mouse and is reported as mean ± SEM. All mice were maintained at the Molecular Biotechnology Center, University of Torino, in specific pathogen-free conditions (Allentown Caging Equipment, Allentown Inc.) and treated in conformity with current European guidelines and policies. The Bioethical Committee of the University of Torino approved the experimental plan.

Cells

TUBO carcinoma cells expressing H-2K^d and Her2/neu are from a mammary carcinoma that arose in a neuT mouse.[51] Cells were cultured in DMEM with Glutamax 1 (DMEM, Life Technologies) supplemented with 20% heat-inactivated fetal bovine serum (FBS; Invitrogen) at 37°C in a humidified 5% CO_2 atmosphere.

Flow cytometry assay for serum antibody detection

Sera collected from BALB/c, neuT and neuT-*C3*$^{-/-}$ mice at different time points were diluted 1:20 in phosphate buffered saline (PBS) with 0.1% sodium azide and 2% bovine serum albumin (BSA, Sigma-Aldrich) (PBS-azide-BSA) and incubated for 30 min at 4°C with 2 × 10^5 TUBO cells pretreated with Fc-receptor blocker (anti-CD16/CD32 antibody; BD Biosciences, 01245B) for 15 min at 4°C. After washing with PBS-azide-BSA, cells were incubated for 30 min with R-phycoerythrin (RPE)-conjugated polyclonal goat anti-mouse IgM (Southern Biotec, 1020–09), washed twice with PBS-azide-BSA and then resuspended in PBS-azide-BSA supplemented with 1 mg/mL of propidium iodide for acquisition. Fluorescence cytometry was performed on a CyAn ADP flow cytometer (DakoCytomation, Beckman Coulter, Milan, Italy). Results were expressed as mean fluorescence intensity (MFI) and analyzed using Summit 4.2 (DakoCytomation) software.

Morphological analyses

The whole mount and immunohistochemical preparation of mammary glands were performed as previously described in detail.[23] Digital pictures were taken with a Nikon Coolpix 995 (Nital, Turin, Italy) mounted on an MZ6 stereoscopic microscope (Leica Microsystems, Milan, Italy). Mammary glands were frozen in a cryo-embedding medium (OCT, Bioptica) for histological and immunohistochemical analyses. Sections were incubated with the following primary antibodies: mouse monoclonal antibodies specific for PCNA (Dako Corporation, M0879); CD105 (550546), CD31 (550274) (both from BD Biosciences); and FoxP3 (eBioscience, 14–5773). Following incubation with primary antibodies and washing steps, appropriate secondary antibodies were applied. Immunocomplexes were detected using Streptavidin Peroxidase (Thermo Scientific-Lab Vision Corporation, Bioptica) and the either DAB Chromogen System (Dako Corporation) or the Bajoran Purple Chromogen System (Biocare Medical); or NeutrAvidin™ Alkaline Phosphatase Conjugated (Thermo Scientific-Pierce Biotechnology, EuroClone) and either Vulcan Fast Red (Biocare Medical) or DAB Chromogen System. The percentage of PCNA$^+$ tumor cells and the number and area of CD31$^+$/CD105$^+$ vessels were evaluated on the digital images of 10 neuT and 10 neuT-*C3*$^{-/-}$ tumors (5 × 400 microscopic fields per tumor) by 2 pathologists, independently and in a blind fashion. Vessels area (in pixels) was evaluated with Adobe Photoshop by selecting vessels with the lasso tool and reporting the number of pixels indicated in the histogram window. Lung samples were fixed in formalin and embedded in paraffin. To optimize the detection of microscopic metastases and ensure systematic uniform and random sampling, lungs were cut transversely, to the trachea, into 2.0-mm-thick parallel slabs with the first cut being in a random position of the first cut in the first 2.0 mm of the lung, resulting in 5–8 slabs per lung. The slabs were then embedded cut surface down. Sections were stained with hematoxylin/eosin and subjected to immunohistochemistry with the anti-Her2 antibody for the evaluation of spontaneous metastasis of all the experimental groups. Metastases were counted independently by 2 pathologists in a blind fashion.

For immunofluorescence analysis cryo-sections were tested with rabbit polyclonal anti-human Her2 (Dako Corporation), rat monoclonal anti-CD105 and anti-CD31 antibodies, all from BD Biosciences, and mouse monoclonal anti-αSMA (Sigma Aldrich), rabbit polyclonal anti-Ng2 (Millipore), hamster anti-mouse-CD31 monoclonal (Chemicon), and rat anti-mouse C3b/iC3b/C3c (HyCult biotech) antibodies. Appropriate Alexafluor-488 and -546 labeled secondary antibodies were then utilized. Nuclei were stained with TO-PRO®-3 Iodide (all from Molecular Probes).

Protein preparation and immunoblotting

Total protein extracts were obtained from mammary glands from 17-week-old neuT and neuT-*C3*$^{-/-}$ mice by using a boiling buffer containing 0.125 M Tris/HCl (pH 6.8) and 2.5% SDS. Her2 expression level was evaluated on whole cell lysates. Thirty μg of proteins were separated by SDS-PAGE and electroblotted onto polyvinylidene fluoride membranes (BioRad). Membranes were blocked in 5% Blotto non-fat milk (Santa Cruz) Tris-buffered saline (TBS)-Tween buffer (137 mM NaCl, 20 mM Tris/HCl, pH 7.6, 0.1% Tween-20) for 1 h at 37°C then incubated with appropriate primary and secondary antibodies in 1% milk TBS-Tween buffer overnight at 4°C and for 1 h at room temperature (RT), respectively, followed by visualization by enhanced chemiluminescence (ECL®, Amersham Biosciences). The following antibodies were used: anti-Her2 (Ab-3) monoclonal antibody (Calbiochem, OP15); anti-actin mouse monoclonal antibody (Santa Cruz, sc-69879), and goat anti-mouse IgG HRP-conjugated (Sigma, A4416). Her2 protein modulation in the mammary glands of neuT-*C3*$^{-/-}$ mice was calculated relative to Her2 mean expression in the mammary glands of neuT mice, normalized on the actin loading control and expressed as percentages using Quantity One software.

Blood collection and C5a and VEGF determination

Blood samples were collected from the retroorbital sinus at the indicated time points from neuT and neuT-*C3*$^{-/-}$ mice, and were allowed to clot for 2 h at RT before centrifugation for 20 min at 1000 × g. Sera were then isolated from the clot and stored at -20°C or -80°C until used. The presence of C5a and VEGF in the sera was determined by commercial ELISA kits specific for C5a, (USCN) and VEGF (R&D), respectively, according to the manufacturer's directions. For VEGF detection, supplied standards were used to generate a standard curve.

Cytofluorometric identification of tumor infiltrating leukocytes

For the phenotypic analysis of tumor-infiltrating cells, fresh primary tumor specimens of 8–10 mm mean diameter from neuT and neuT-*C3*$^{-/-}$ mice were finely minced with scissors and then digested by incubation with 1 mg/mL collagenase IV (Sigma Aldrich) in RPMI-1640 (Life Technologies) at 37°C for 1 h in an orbital shaker. After washing in PBS supplemented with 2% fetal calf serum (GIBCO), the cell suspension was incubated in erylise buffer (155 mM NH_4Cl, 15.8 mM Na_2CO_3, 1 mM EDTA, pH 7.3) for 10 min at RT. After washing in RPMI-1640 supplemented with 10% FBS, the cell suspension was passed through a 70-μm pore cell strainer, centrifuged at 1400 rpm for 10 min and resuspended in erylise buffer. Cells were collected, washed, re-suspended in PBS, treated with Fc-receptor blocker, and stained with the following antibodies: anti-mouse CD3e PerCP, (553067), anti-mouse CD11b APC-Cy7 (557657), anti-mouse Ly-6G and Ly-6C FITC (551460), anti-mouse B220 Pacific blue (558108) all from BD Biosciences; anti-mouse CD4 PE/Cy7 (100528) and anti-mouse F/480 PE (122615) from BioLegend; anti-mouse CD45 APC (130–091–811) (Miltenyi Biotech); anti-mouse CD8 FITC (11–0081–86) and anti-mouse CD25 APC (102012) (eBioscience). To detect FoxP3$^+$ T regulatory cells, samples were permeabilized with the FoxP3 anti mouse staining kit (eBioscience) and stained with anti-mouse/rat-Foxp3-FITC antibody (FJK-16s; eBioscience). Samples were acquired on the CyAn ADP cytofluorometer and analyzed using the Summit 4.3 software.

Isolation of tumor cells from primary carcinoma specimens and transplantation

Primary tumor specimens obtained from 8–10 mm mean diameter spontaneous mammary carcinomas developed in neuT and neuT-*C3*$^{-/-}$ mice (each time 2–4 spontaneous tumors from the same mouse; n = 5) were finely minced with scissors and then digested by incubation with 1 mg/mL collagenase IV in RPMI-1640 (Life Technologies) at 37°C for 1 h in an orbital shaker. After washing in PBS supplemented with 2% FBS, the cell suspension was incubated in erylise buffer for 10 min at RT and then washed twice with cold PBS. Cell pellets were re-suspended in Trypsin supplemented with 0.05% EDTA for 15 min at 37°C and disaggregated with a serological pipette. Cancer cells were then washed once in PBS supplemented with 2% FBS, passed through a 70 μm pore cell strainer to separate the cell components from stroma and aggregates, and re-suspended in endotoxin-free PBS. One million viable cells were injected subcutaneously into the flank of wild type or *C3*$^{-/-}$ BALB/c mice. Tumor growth was monitored weekly as described above.

Dynamic contrast-enhanced magnetic resonance imaging (DCE-MRI)

Magnetic resonance images were acquired on anesthetized mice using an Aspect M2 MRI System (Aspect Magnet Technologies Ltd., Netanya, Israel) working at 1 Tesla. Mice were placed supine inside a solenoid Tx/Tr coil with an inner diameter of 3.5 cm. A phantom filled with diluted ProHance (Bracco Imaging SpA) was included in the field of view (FOV), close to each animal, to allow correction for potential spectrometer variation. After the scout image was acquired, a T_2-weighted (w) anatomical image was obtained using a Fast Spin Echo sequence (TR 2500 s; TE 41 msec; number of slices 8; slice thickness 1.5 mm; FOV 40 mm; matrix 128 x 128; 4 averages; acquisition time 2 min 40 s). The baseline tumor T_1 map was acquired by using a variable flip-angle Gradient-Echo (VFA-GRE) sequence (7 flip angles in the range 15°-160°). The DCE-MRI dynamic protocol was performed using an axial T_{1w} 3D spoiled Gradient Echo sequence with 3 initial pre-contrast images and 47 dynamic post-contrast images with the following parameters: TR/TE = 40/1.8 msec, flip angle = 60°, number of slices = 10, slice thickness = 1.5 mm, FOV = 40 mm, matrix = 128 × 128. The gadolinium-containing serum albumin binding contrast agent (Phenoquant, Cage Chemicals) was injected into the tail vein of neuT (n = 2) and neuT-*C3*$^{-/-}$ (n = 4) mice bearing 6-mm mean diameter autochthonous mammary tumors in the IV mammary glands, at a dose of 0.05 mmol Gd/kg.

The acquired raw DCE-MRI data were analyzed using a quantitative method and by implementing a 2-compartment extended Tofts model on in-house developed C++ software, which yielded the relevant parametric maps (Ktrans and Vp).[52] Diffusion weighted images (DWI) were acquired by using a Spin-Echo sequence with 7 b-values between 0 and 600 s/mm^2. ADCs (mm^2/sec) were calculated by fitting the obtained images as a function of b-values on a pixel-by-pixel basis.

Statistical analyses

Tumor incidence was compared using the Log-rank Mantel-Cox test. All other data sets were analyzed for statistical significance with 2-tailed Student's t-tests.

Disclosure of Potential Conflicts of Interest

No potential conflicts of interest were disclosed.

Acknowledgments

This work was supported by grants from the Italian Association for Cancer Research (IG 11675), Fondazione Ricerca Molinette Onlus, the University of Torino, and the Compagnia di San Paolo (Progetti di Ricerca Ateneo/CSP). We thank Dr. Dale Lawson for his revision and editing of the manuscript.

Supplemental Materials

Supplemental materials may be found here:
www.landesbioscience.com/journals/oncoimmunology/article/26137

References

1. Colotta F, Allavena P, Sica A, Garlanda C, Mantovani A. Cancer-related inflammation, the seventh hallmark of cancer: links to genetic instability. Carcinogenesis 2009; 30:1073-81; PMID:19468060; http://dx.doi.org/10.1093/carcin/bgp127
2. Balkwill F, Mantovani A. Inflammation and cancer: back to Virchow? Lancet 2001; 357:539-45; PMID:11229684; http://dx.doi.org/10.1016/S0140-6736(00)04046-0
3. Dunn GP, Old LJ, Schreiber RD. The immunobiology of cancer immunosurveillance and immunoediting. Immunity 2004; 21:137-48; PMID:15308095; http://dx.doi.org/10.1016/j.immuni.2004.07.017
4. Schreiber RD, Old LJ, Smyth MJ. Cancer immunoediting: integrating immunity's roles in cancer suppression and promotion. Science 2011; 331:1565-70; PMID:21436444; http://dx.doi.org/10.1126/science.1203486

5. Vesely MD, Kershaw MH, Schreiber RD, Smyth MJ. Natural innate and adaptive immunity to cancer. Annu Rev Immunol 2011; 29:235-71; PMID:21219185; http://dx.doi.org/10.1146/annurev-immunol-031210-101324
6. Fujita T, Taira S, Kodama N, Matsushita M, Fujita T. Mannose-binding protein recognizes glioma cells: in vitro analysis of complement activation on glioma cells via the lectin pathway. Jpn J Cancer Res 1995; 86:187-92; PMID:7730143; http://dx.doi.org/10.1111/j.1349-7006.1995.tb03038.x
7. Swierzko AS, Kilpatrick DC, Cedzynski M. Mannan-binding lectin in malignancy. Mol Immunol 2013; 55:16-21; PMID:23062612; http://dx.doi.org/10.1016/j.molimm.2012.09.005
8. Gao LJ, Gu PQ, Fan WM, Liu Z, Qiu F, Peng YZ, Guo XR. The role of gC1qR in regulating survival of human papillomavirus 16 oncogene-transfected cervical cancer cells. Int J Oncol 2011; 39:1265-72; PMID:21725590
9. Vollmers HP, Brändlein S. Natural antibodies and cancer. N Biotechnol 2009; 25:294-8; PMID:19442595; http://dx.doi.org/10.1016/j.nbt.2009.03.016
10. Hamaï A, Duperrier-Amouriaux K, Pignon P, Raimbaud I, Memeo L, Colarossi C, Canzonieri V, Perin T, Classe JM, Campone M, et al. Antibody responses to NY-ESO-1 in primary breast cancer identify a subtype target for immunotherapy. PLoS One 2011; 6:e21129; PMID:21747904; http://dx.doi.org/10.1371/journal.pone.0021129
11. Lu H, Ladd J, Feng Z, Wu M, Goodell V, Pitteri SJ, Li CI, Prentice R, Hanash SM, Disis ML. Evaluation of known oncoantibodies, HER2, p53, and cyclin B1, in prediagnostic breast cancer sera. Cancer Prev Res (Phila) 2012; 5:1036-43; PMID:22715141; http://dx.doi.org/10.1158/1940-6207.CAPR-11-0558
12. Stover C. Dual role of complement in tumour growth and metastasis (Review). [Review]. Int J Mol Med 2010; 25:307-13; PMID:20127033; http://dx.doi.org/10.3892/ijmm_00000346
13. Ricklin D, Hajishengallis G, Yang K, Lambris JD. Complement: a key system for immune surveillance and homeostasis. Nat Immunol 2010; 11:785-97; PMID:20720586; http://dx.doi.org/10.1038/ni.1923
14. Nunez-Cruz S, Gimotty PA, Guerra MW, Connolly DC, Wu YQ, DeAngelis RA, Lambris JD, Coukos G, Scholler N. Genetic and pharmacologic inhibition of complement impairs endothelial cell function and ablates ovarian cancer neovascularization. Neoplasia 2012; 14:994-1004; PMID:23226093
15. Green JE, Hudson T. The promise of genetically engineered mice for cancer prevention studies. Nat Rev Cancer 2005; 5:184-98; PMID:15738982; http://dx.doi.org/10.1038/nrc1565
16. Lollini PL, Cavallo F, Nanni P, Forni G. Vaccines for tumour prevention. Nat Rev Cancer 2006; 6:204-16; PMID:16498443; http://dx.doi.org/10.1038/nrc1815
17. Cavallo F, Offringa R, van der Burg SH, Forni G, Melief CJ. Vaccination for treatment and prevention of cancer in animal models. Adv Immunol 2006; 90:175-213; PMID:16730264; http://dx.doi.org/10.1016/S0065-2776(06)90005-4
18. Quaglino E, Mastini C, Forni G, Cavallo F. ErbB2 transgenic mice: a tool for investigation of the immune prevention and treatment of mammary carcinomas. Curr Protoc Immunol 2008; Chapter 20:Unit 20 9 1- 9-10.
19. Conti L, Lanzardo S, Iezzi M, Montone M, Bolli E, Brioschi C, Maiocchi A, Forni G, Cavallo F. Optical imaging detection of microscopic mammary cancer in ErbB-2 transgenic mice through the DA364 probe binding αv β3 integrins. Contrast Media Mol Imaging 2013; 8:350-60; PMID:23613438; http://dx.doi.org/10.1002/cmmi.1529
20. Hüsemann Y, Geigl JB, Schubert F, Musiani P, Meyer M, Burghart E, Forni G, Eils R, Fehm T, Riethmüller G, et al. Systemic spread is an early step in breast cancer. Cancer Cell 2008; 13:58-68; PMID:18167340; http://dx.doi.org/10.1016/j.ccr.2007.12.003
21. Sangaletti S, Tripodo C, Ratti C, Piconese S, Porcasi R, Salcedo R, Trinchieri G, Colombo MP, Chiodoni C. Oncogene-driven intrinsic inflammation induces leukocyte production of tumor necrosis factor that critically contributes to mammary carcinogenesis. Cancer Res 2010; 70:7764-75; PMID:20924115; http://dx.doi.org/10.1158/0008-5472.CAN-10-0471
22. Coscia M, Quaglino E, Iezzi M, Curcio C, Pantaleoni F, Riganti C, Holen I, Mönkkönen H, Boccadoro M, Forni G, et al. Zoledronic acid repolarizes tumour-associated macrophages and inhibits mammary carcinogenesis by targeting the mevalonate pathway. J Cell Mol Med 2010; 14:2803-15; PMID:19818098; http://dx.doi.org/10.1111/j.1582-4934.2009.00926.x
23. Street SE, Zerafa N, Iezzi M, Westwood JA, Stagg J, Musiani P, Smyth MJ. Host perforin reduces tumor number but does not increase survival in oncogene-driven mammary adenocarcinoma. Cancer Res 2007; 67:5454-60; PMID:17545627; http://dx.doi.org/10.1158/0008-5472.CAN-06-4084
24. Rolla S, Ria F, Occhipinti S, Di Sante G, Iezzi M, Spadaro M, Nicolò C, Ambrosino E, Merighi IF, Musiani P, et al. Erbb2 DNA vaccine combined with regulatory T cell deletion enhances antibody response and reveals latent low-avidity T cells: potential and limits of its therapeutic efficacy. J Immunol 2010; 184:6124-32; PMID:20435927; http://dx.doi.org/10.4049/jimmunol.0901215
25. Ambrosino E, Spadaro M, Iezzi M, Curcio C, Forni G, Musiani P, Wei WZ, Cavallo F. Immunosurveillance of Erbb2 carcinogenesis in transgenic mice is concealed by a dominant regulatory T-cell self-tolerance. Cancer Res 2006; 66:7734-40; PMID:16885376; http://dx.doi.org/10.1158/0008-5472.CAN-06-1432
26. Spadaro M, Ambrosino E, Iezzi M, Di Carlo E, Sacchetti P, Curcio C, Amici A, Wei WZ, Musiani P, Lollini PL, et al. Cure of mammary carcinomas in Her-2 transgenic mice through sequential stimulation of innate (neoadjuvant interleukin-12) and adaptive (DNA vaccine electroporation) immunity. Clin Cancer Res 2005; 11:1941-52; PMID:15756020; http://dx.doi.org/10.1158/1078-0432.CCR-04-1873
27. Calogero RA, Cordero F, Forni G, Cavallo F. Inflammation and breast cancer. Inflammatory component of mammary carcinogenesis in ErbB2 transgenic mice. Breast Cancer Res 2007; 9:211; PMID:17705881; http://dx.doi.org/10.1186/bcr1745
28. Strainic MG, Shevach EM, An F, Lin F, Medof ME. Absence of signaling into CD4+ cells via C3aR and C5aR enables autoinductive TGF-β1 signaling and induction of Foxp3+ regulatory T cells. Nat Immunol 2013; 14:162-71; PMID:23263555; http://dx.doi.org/10.1038/ni.2499
29. Kwan WH, van der Touw W, Paz-Artal E, Li MO, Heeger PS. Signaling through C5a receptor and C3a receptor diminishes function of murine natural regulatory T cells. J Exp Med 2013; 210:257-68; PMID:23382542; http://dx.doi.org/10.1084/jem.20121525
30. Langer HF, Chung KJ, Orlova VV, Choi EY, Kaul S, Kruhlak MJ, Alatsatianos M, DeAngelis RA, Roche PA, Magotti P, et al. Complement-mediated inhibition of neovascularization reveals a point of convergence between innate immunity and angiogenesis. Blood 2010; 116:4395-403; PMID:20625009; http://dx.doi.org/10.1182/blood-2010-01-261503
31. Melani C, Chiodoni C, Forni G, Colombo MP. Myeloid cell expansion elicited by the progression of spontaneous mammary carcinomas in c-erbB-2 transgenic BALB/c mice suppresses immune reactivity. Blood 2003; 102:2138-45; PMID:12750171; http://dx.doi.org/10.1182/blood-2003-01-0190
32. Brunn GJ, Saadi S, Platt JL. Constitutive repression of interleukin-1alpha in endothelial cells. Circ Res 2008; 102:823-30; PMID:18292602; http://dx.doi.org/10.1161/CIRCRESAHA.107.165332
33. Muto S, Sakuma K, Taniguchi A, Matsumoto K. Human mannose-binding lectin preferentially binds to human colon adenocarcinoma cell lines expressing high amount of Lewis A and Lewis B antigens. Biol Pharm Bull 1999; 22:347-52; PMID:10328552; http://dx.doi.org/10.1248/bpb.22.347
34. Halperin JA, Taratuska A, Nicholson-Weller A. Terminal complement complex C5b-9 stimulates mitogenesis in 3T3 cells. J Clin Invest 1993; 91:1974-8; PMID:8486768; http://dx.doi.org/10.1172/JCI116418
35. Reiter Y, Ciobotariu A, Fishelson Z. Sublytic complement attack protects tumor cells from lytic doses of antibody and complement. Eur J Immunol 1992; 22:1207-13; PMID:1577063; http://dx.doi.org/10.1002/eji.1830220515
36. Markiewski MM, DeAngelis RA, Benencia F, Ricklin-Lichtsteiner SK, Koutoulaki A, Gerard C, Coukos G, Lambris JD. Modulation of the antitumor immune response by complement. Nat Immunol 2008; 9:1225-35; PMID:18820683; http://dx.doi.org/10.1038/ni.1655
37. Gunn L, Ding C, Liu M, Ma Y, Qi C, Cai Y, Hu X, Aggarwal D, Zhang HG, Yan J. Opposing roles for complement component C5a in tumor progression and the tumor microenvironment. J Immunol 2012; 189:2985-94; PMID:22914051; http://dx.doi.org/10.4049/jimmunol.1200846
38. Schwartz-Albiez R, Laban S, Eichmüller S, Kirschfink M. Cytotoxic natural antibodies against human tumours: an option for anti-cancer immunotherapy? Autoimmun Rev 2008; 7:491-5; PMID:18558368; http://dx.doi.org/10.1016/j.autrev.2008.03.012
39. Quaglino E, Rolla S, Iezzi M, Spadaro M, Musiani P, De Giovanni C, Lollini PL, Lanzardo S, Forni G, Sanges R, et al. Concordant morphologic and gene expression data show that a vaccine halts HER-2/neu preneoplastic lesions. J Clin Invest 2004; 113:709-17; PMID:14991069
40. Porzia A, Lanzardo S, Citti A, Cavallo F, Forni G, Santoni A, Galandrini R, Paolini R. Attenuation of PI3K/Akt-mediated tumorigenic signals through PTEN activation by DNA vaccine-induced anti-ErbB2 antibodies. J Immunol 2010; 184:4170-7; PMID:20220087; http://dx.doi.org/10.4049/jimmunol.0903375
41. Spendlove I, Ramage JM, Bradley R, Harris C, Durrant LG. Complement decay accelerating factor (DAF)/CD55 in cancer. Cancer Immunol Immunother 2006; 55:987-95; PMID:16485129; http://dx.doi.org/10.1007/s00262-006-0136-8
42. Vêtvicka V, Hanikýrová M, Vêtvicková J, Ross GD. Regulation of CR3 (CD11b/CD18)-dependent natural killer (NK) cell cytotoxicity by tumour target cell MHC class I molecules. Clin Exp Immunol 1999; 115:229-35; PMID:9933447; http://dx.doi.org/10.1046/j.1365-2249.1999.00800.x
43. Inoue M, Mimura K, Izawa S, Shiraishi K, Inoue A, Shiba S, Watanabe M, Maruyama T, Kawaguchi Y, Inoue S, et al. Expression of MHC Class I on breast cancer cells correlates inversely with HER2 expression. Oncoimmunology 2012; 1:1104-10; PMID:23170258; http://dx.doi.org/10.4161/onci.21056
44. Okita R, Mougiakakos D, Ando T, Mao Y, Sarhan D, Wennerberg E, Seliger B, Lundqvist A, Mimura K, Kiessling R. HER2/HER3 signaling regulates NK cell-mediated cytotoxicity via MHC class I chain-related molecule A and B expression in human breast cancer cell lines. J Immunol 2012; 188:2136-45; PMID:22301547; http://dx.doi.org/10.4049/jimmunol.1102237

45. Strainic MG, Liu J, Huang D, An F, Lalli PN, Muqim N, Shapiro VS, Dubyak GR, Heeger PS, Medof ME. Locally produced complement fragments C5a and C3a provide both costimulatory and survival signals to naive CD4+ T cells. Immunity 2008; 28:425-35; PMID:18328742; http://dx.doi.org/10.1016/j.immuni.2008.02.001
46. Amara U, Flierl MA, Rittirsch D, Klos A, Chen H, Acker B, Brückner UB, Nilsson B, Gebhard F, Lambris JD, et al. Molecular intercommunication between the complement and coagulation systems. J Immunol 2010; 185:5628-36; PMID:20870944; http://dx.doi.org/10.4049/jimmunol.0903678
47. Huber-Lang M, Sarma JV, Zetoune FS, Rittirsch D, Neff TA, McGuire SR, Lambris JD, Warner RL, Flierl MA, Hoesel LM, et al. Generation of C5a in the absence of C3: a new complement activation pathway. Nat Med 2006; 12:682-7; PMID:16715088; http://dx.doi.org/10.1038/nm1419
48. O'Sullivan T, Saddawi-Konefka R, Vermi W, Koebel CM, Arthur C, White JM, Uppaluri R, Andrews DM, Ngiow SF, Teng MW, et al. Cancer immunoediting by the innate immune system in the absence of adaptive immunity. J Exp Med 2012; 209:1869-82; PMID:22927549; http://dx.doi.org/10.1084/jem.20112738
49. Corrales L, Ajona D, Rafail S, Lasarte JJ, Riezu-Boj JI, Lambris JD, Rouzaut A, Pajares MJ, Montuenga LM, Pio R. Anaphylatoxin C5a creates a favorable microenvironment for lung cancer progression. J Immunol 2012; 189:4674-83; PMID:23028051; http://dx.doi.org/10.4049/jimmunol.1201654
50. Trendelenburg M, Fossati-Jimack L, Cortes-Hernandez J, Turnberg D, Lewis M, Izui S, Cook HT, Botto M. The role of complement in cryoglobulin-induced immune complex glomerulonephritis. J Immunol 2005; 175:6909-14; PMID:16272350
51. Rovero S, Amici A, Di Carlo E, Bei R, Nanni P, Quaglino E, Porcedda P, Boggio K, Smorlesi A, Lollini PL, et al. DNA vaccination against rat her-2/Neu p185 more effectively inhibits carcinogenesis than transplantable carcinomas in transgenic BALB/c mice. J Immunol 2000; 165:5133-42; PMID:11046045
52. Arigoni M, Barutello G, Lanzardo S, Longo D, Aime S, Curcio C, Iezzi M, Zheng Y, Barkefors I, Holmgren L, et al. A vaccine targeting angiomotin induces an antibody response which alters tumor vessel permeability and hampers the growth of established tumors. Angiogenesis 2012; 15:305-16; PMID:22426512; http://dx.doi.org/10.1007/s10456-012-9263-3